Right Aortic Arch with Mirror-image Branching in Adults: Evaluation Using CT

Toshihiko HAYASHI[*1], Tamaki ICHIKAWA[*1], Hiroshi YAMAMURO[*1], Shun ONO[*1], Makiko KOBAYASHI[*1, 2], Takakiyo NOMURA[*1], Kazunobu HASHIDA[*5], Hideki YASHIRO[*2], Tomohisa OKOCHI[*3], Jun KOIZUMI[*1], Shinichiro SHIMURA[*4], Terumitsu HASEBE[*5] and Yutaka IMAI[*1]

[*1]*Department of Radiology, Tokai University School of Medicine*
[*2]*Division of Diagnostic Radiology, Hiratsuka City Hospital*
[*3]*Department of Radiology, Jichi Medical University Saitama Medical Center*
[*4]*Department of Cardiovascular Surgery, Tokai University School of Medicine*
[*5]*Department of Radiology, Tokai University Hachioji Hospital, Tokai University School of Medicine*

(Received January 24, 2018; Accepted February 19, 2018)

Objective: We evaluated radiological findings and clinical significance of right aortic arch with mirror-image branching (RAMI) in adults using data from computed tomography (CT) examinations.
Material and methods: We reviewed recorded reports and CT images obtained from university and branch hospitals for RAMI in adults. The RAMI incidence in adults found on CT was assessed. Associated congenital and acquired cardiovascular diseases were evaluated.
Results: A total of 27 cases (14 men, 13 women; mean age, 59.4 ± 18.3 years) of RAMI were found. Among 107,014 cases in three hospitals, the RAMI incidence in the first, second, and third Tokai University hospitals were 0.018%, 0.012%, and 0.012%, respectively. Eight cases had high aortic arches and four cases had aortic diverticulum (AD) in proximal descending aorta. Three cases had a history of tetralogy of Fallot. One case with an absent left pulmonary artery and three cases with an aberrant left brachiocephalic vein were found incidentally. Two cases were associated with AD aneurysm and vascular ring formation. One case had stenosis of the left subclavian artery due to injury.
Conclusion: Cases of RAMI found in CT examinations in adults were extremely rare. Some cases were associated with congenital anomalies and/or acquired cardiovascular disease.

Key words: right aortic arch, mirror-image branching, computed tomography, adult

INTRODUCTION

Congenital anomalies of the aortic arch are not common, with frequencies ranging from 0.5% to 3.0% [1–3]. Among these, right aortic arch (RAA) is a rare congenital variant in vascular anatomy. In radiographic and autopsy studies, RAA has been found in approximately 1 out of 1000 individuals [2, 4–12]. A variety of patterns of brachiocephalic vessel branching are seen in the context of RAA. Several classifications of this anomaly have been described [5, 13–15]. Edwards *et al*. [14, 15] classified the following types of RAA. The most common pattern is RAA with aberrant left subclavian artery with or without a remnant of the left dorsal aortic root (Kommerell's diverticulum) (type IIIB) [2, 14–16]. RAA with mirror-image branching (RAMI) is the second most common type of RAA (type IIIA) [2, 14–16]. RAA with aberrant left brachiocephalic artery and RAA with isolated left subclavian artery are rare anomalies (type IIIC) [2, 14–16].

Among these congenital RAA anomalies, almost all cases of RAMI have been detected during childhood, and found to be associated with concomitant congenital heart disease (CHD) in approximately 98% of patients [2, 11, 13, 16, 17]. RAMI is typically found in conjunction with cardiac anomalies such as tetralogy of Fallot (TOF), pulmonary atresia, or truncus arteriosus [2, 6, 17, 18]. Because of the significant association with CHD, cardiac morphology and RAA almost always appear abnormal in imaging [2]. Therefore, many studies of RAMI in fetuses, neonates, infants, and children have been reported [6, 13, 17–22].

However, several RAMI cases in adults without CHD have been reported [7–10, 12, 23–25]. Such cases of RAMI are usually found in asymptomatic patients, and rarely in cases with vascular rings that encircle the trachea and esophagus and/or with acquired aortic diseases such as dissection and aneurysmal dilation. A few RAMI cases with symptomatic vascular ring have also been reported in adults with dilated aortic diverticulum (AD) [8, 12, 24, 25]. In rare variants of RAMI, the descending aorta courses on the left side of the spine. This variant might be associated with a vascular ring with retroesophageal AD connecting to the left ductus arteriosus or ligamentum arteriosum [19, 24]. Symptomatic RAMI cases caused by acquired aortic diseases such as dissection or aneurysmal dilation with compression of surrounding structures and without

Yutaka IMAI, Department of Radiology, Tokai University School of Medicine, 143 Shimokasuya, Isehara, kanagawa 259-1193, Japan
Tel: +81-463-93-1121 Fax: +81-463-03-6827 E-mail: imaiy@is.icc.u-tokai.ac.jp

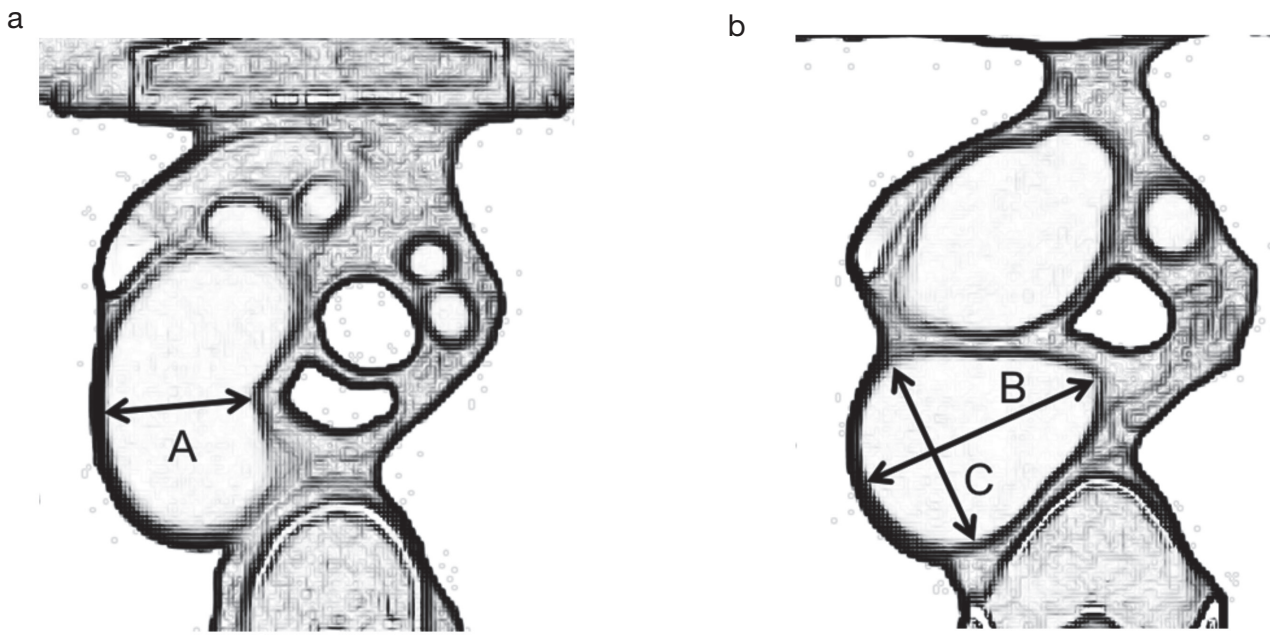

Fig. 1 Definition of measuring points in a RAMI case with aortic diverticulum in a schematic drawing.
Two measurement points on axial images were defined. (a) Short diameter in the aortic arch = A, (b) long and short diameter in the proximal descending aorta = B and C, respectively. Aortic bump: $1 < B/A < 1.5$, aortic diverticulum: $1.5 \leq B/A < 2$, aortic aneurysm: $2 \leq B/A$ or $1.5 \leq B/A$ and $1.5 \leq C/A$.

vascular ring have been reported in adults [7, 9, 10, 23].

To our knowledge, clinical significance and incidence of RAMI in adults have not been explored. We aimed to evaluate radiologic findings and clinical significance of RAMI in adults detected in computed tomography (CT) examinations.

MATERIAL AND METHODS

The all institutional ethics committee of Tokai University hospitals and the other branch hospital groups approved this retrospective study and granted a waiver for the requirement of informed consent.

To assess the incidence of RAMI in adults found using CT, we reviewed CT examinations conducted in three university groups. The groups were designated as the first, second, and third university hospital groups. Adults in the first university hospital group underwent chest CT examinations between January 2006 and October 2016, and those in the second university hospital group underwent chest CT examinations between January 2003 and October 2016. From the chest CT reports in the first and second university hospital groups, cases with RAMI were identified using searches with the keywords "RAA," "RAMI," "double aortic arch," or "incomplete double aortic arch (IDA)." In the third university hospital group, we reviewed all CT images to search for RAMI between January 2006 and October 2016. All cases in adults 20 years or older were selected in three university hospital groups. When more than two cases were found in each group, the incidences of RAMI were compared using Fisher's exact test. We compared demographic data between the groups using the chi-square test and Mann-Whitney test. Statistical analysis was performed with the software SPSS version 23. P values less than 0.05 were considered significant.

For evaluation of clinical significance of RAMI in adults detected using CT, the above cases from the three university hospitals and those from two other branch hospitals were included. CT was performed using a 16- to 320-slice scanner (Somatom Sensation Cardiac 64, Definition, Definition Flash, Definition Edge, Definition AS+; Siemens AG, Munich, Germany, Aquilion, or Aquilion one; Canon Medical System, Otawara, Japan) at a slice thickness of 0.5 mm. The other parameters were as follows: tube voltage, 70−150 kVp; tube current, auto mA; and rotation time, 0.5 s. Contrast-enhanced CT examinations were performed by injecting 2 mL/kg of nonionic contrast material at a rate of 2 mL/s with a 120-s scanning delay. CT angiography was performed using the bolus tracking method after an infusion of 2 mL/kg of nonionic contrast material at rate of 4 mL/s.

Two radiologists, each with more than 10 years of experience in CT image interpretation, reviewed the 1−5 mm reconstructed axial CT images on a picture archiving and communication system workstation. If needed, additional multiplanar reformations and volume-rendering images were used for the evaluations. They assessed the presence or absence of AD in the proximal descending aorta. When AD in the proximal descending aorta was found, we used D'Souza's and Schlesingers' criteria for distinguishing RAMI from IDA (Table 1) [19, 26]. We defined a slight protrusion of aortic wall in the proximal descending aorta as an aortic bump. We used the definition (Fig. 1) for distinguishing AD from aortic bump and aortic aneurysm. The aortic arch level was evaluated, and if the arch was seen above the lower margin of the clavicle, we considered it to be a high aortic arch [27]. Associated congenital or acquired cardiovascular diseases were assessed using CT images and medical records. The radiologists resolved any disagreement through consensus.

Table 1 Differentiation between RAMI and IDA: adapted from D'Souza VJ [19] and Schlesinger AE [26].

	RAMI	IDA
AD	(+) or (-)	(+)
Shape of AD	Round, conical	Round, conical, or long tubular
Branches of aortic arch	Asymmetric	Symmetric
Position of LCA	Anterior	Posterior
Coursing of DA	AD (-): PA to LSA	PA to LSA
	AD (+): PA to AD	PA to AD
DA attachment point in AD	Laterally or posteriorly	Anteriorly

RAMI right aortic arch with mirror-image branching, *IDA* incomplete double aortic arch, *DA* ductus arteriosus, *PA* pulmonary artery, *AD* aortic diverticulum, *LSA* left subclavian artery, *LCA* left common carotid artery

RESULTS

Total 107,014 CT examinations in three university hospital groups were evaluated to determine the RAMI incidence. In the first university hospital group, 73,800 cases underwent CT examinations during the study period (42,755 men and 31,045 women; mean age, 62.3 ± 16.2 years). In the second university hospital group, 25,189 cases underwent CT examinations during the study period (14,200 men and 10,989 women; mean age 61.8 ± 19.8 years). In the third university hospital group, 8025 cases underwent CT examinations during the study period (5133 men and 2892 women; mean age, 62.3 ± 16.2 years).

In the first university hospital group, 14 cases with RAMI were found; nine of these were men and five were women, with a mean age of 59.1 ± 18.6 years and a RAMI incidence of 0.018%. In the second university hospital group, five cases had RAMI; two were men and three were women, with a mean age of 67.4 ± 24.4 years and a RAMI incidence of 0.012%. In the third university hospital group, one case had RAMI and a RAMI incidence of 0.012%. No significant differences were observed in demographic data between the first and second hospital groups (age: $p = 0.18$, sex: $p = 0.20$). No significant differences were observed in RAMI incidence between the first and second hospital groups ($p = 0.49$).

Considering five hospitals including the three large university hospitals above, a total of 27 cases of RAMI were found; 14 of these were men and 13 were women, with a mean age of 59.4 ± 18.3 years (Table 2). Seven cases were found in non-contrast CT, and 20 cases were identified through contrast-enhanced CT including seven CT angiographic examinations. Twenty-three cases had a right-sided descending aorta (85%) and in four cases, the descending aorta presented midline to the spine (15%). Eight cases had high aortic arches (30%).

Four cases with right-sided descending aorta had AD (17%) and none of the AD cases were associated with CHD. Shapes of the AD were either round or conical. Two cases had symptomatic AD; one was a chronic dissecting aneurysm, which was the largest AD found with a diameter of 72 mm (Fig. 2, Table 2), and the other was an AD aneurysm (Fig. 3, Table 2). The latter AD aneurysm case underwent aortic repair and during surgery, ductus arteriosus was found attached to the AD posteriorly. Both cases showed vascular ring formation due to complicated AD. In two other cases with asymptomatic AD, loose attachment of ductus arteriosus to the AD was seen. Among four cases with a midline descending aorta, three had an aortic bump in the left portion of the descending aorta proximal to the esophagus (Fig. 4, Table 2).

A total of five RAMI cases were associated with congenital cardiovascular anomalies and none of these cases had AD. Three cases had a status of post-operative TOF. Three cases had an aberrant left brachiocephalic vein (ALBCV). Two of the three cases with TOF were associated with ALBCV (Fig. 5, Table 2), and one of them had patent foramen ovale. One case associated with congenital absence of the left pulmonary artery was found incidentally (Fig. 6, Table 2). One case had left ductus arteriosus between the proximal left pulmonary artery and the left brachiocephalic artery. One case was associated with horseshoe kidney. CTA revealed that a young female had chronic stenosis of the proximal left subclavian artery with subclavian steal syndrome due to injury. She has been planning to undergo axillo-axillary bypass.

DISCUSSION

A study by Edwards has discussed developmental errors and variations in the aortic arch [14, 15]. If the distal portion of the left aortic arch adjacent to the descending aorta disappears, subsequent development results in RAMI [6, 16].

In previous studies, almost all RAMI cases were found to be associated with CHD, and especially with TOF [2, 6, 17, 18]. RAMI cases with CHD typically have no AD [6, 13, 17, 18, 21]. In our study, RAMI cases detected in CT examinations comprised three cases of post-operative TOF, one case of absent left pulmonary artery, and 22 cases without major congenital cardiovascular disease. None of the three RAMI cases with post-operative TOF had AD. This was consistent with several previous studies.

In cases with normal left aortic arch (LAA), aneurysms in the descending thoracic aorta often result from atherosclerosis and typically originate in the proximal descending aorta wall [28]. Further, in aortic dissection cases with normal LAA, the entry tear often occurs close to the site of the ligamentum arteriosum in the descending aorta (Stanford type B dissection) [29, 30]. Based on the above findings, it has been suggested that effects of blood flow and pressure may be significantly felt in the proximal descending aorta.

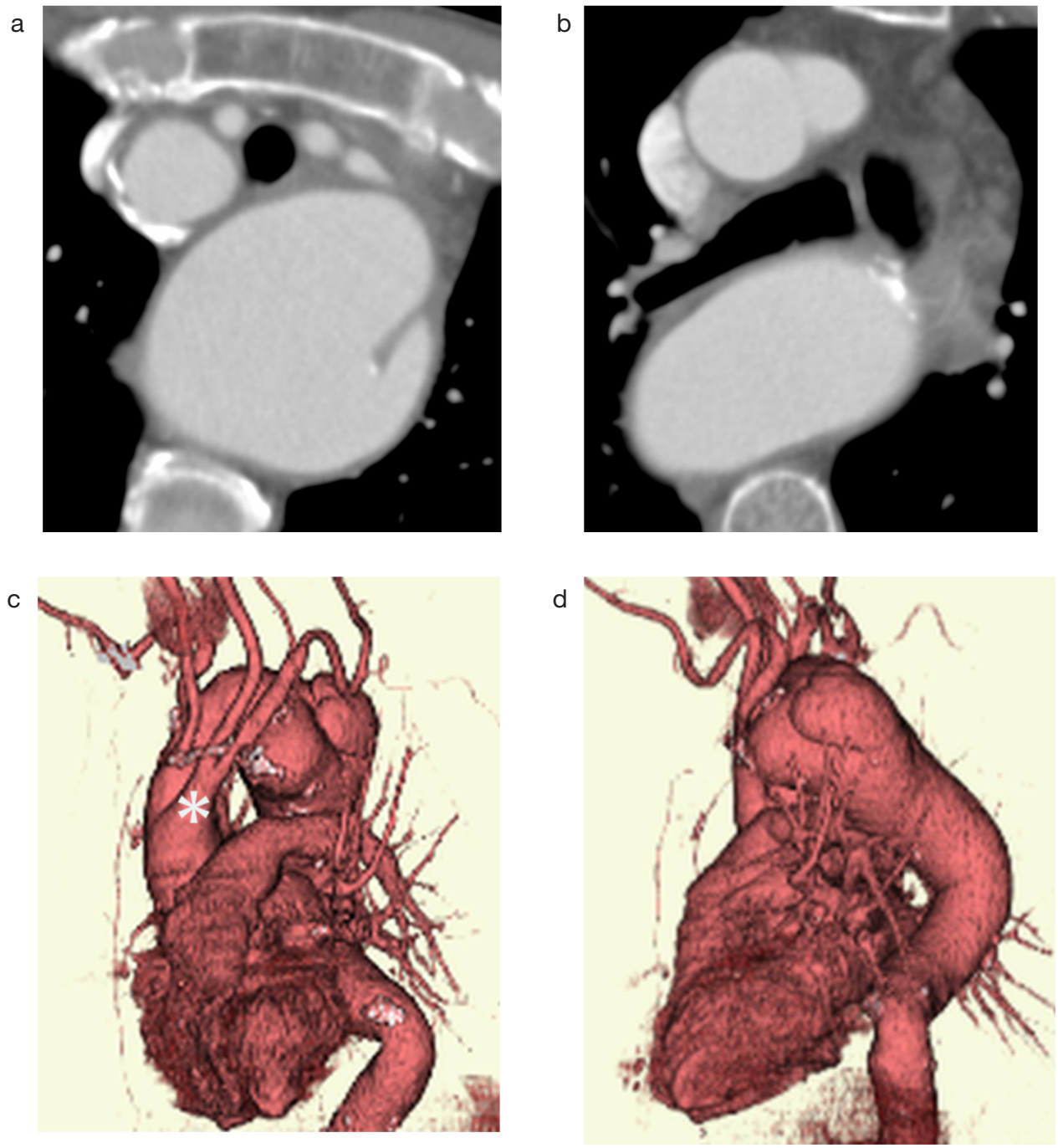

Fig. 2 CT images of a dissecting aneurysm involving aortic diverticulum in a 76-year-old male (no. 11 in Table 2). (a, b) Axial image showing a dissecting aneurysm involving aortic diverticulum. (c) A left anterior oblique view of a three-dimensional (3D) image showing the RAMI and Stanford type-B dissection. The asterisk shows the left brachiocephalic artery. (d) A left posterior oblique view of the 3D image showing an aortic diverticulum in the proximal descending aorta with dissecting aneurysm.

A recent study has explored the effect of blood flow on the aortic wall using computational fluid dynamics (CFD) and found high mechanical stress exerted on the proximal descending aorta [31].

Cases of RAA including RAMI might have a higher potential risk of acquired aortic disease such as dissection or aneurysm due to abnormal blood flow and pressure compared with cases of LAA [32]. RAA results in a shorter radius and more acute curvature of the aortic arch compared to the gentler gradient curve in LAA, and this may be an additional factor contributing to stress on the proximal descending aortic wall, leading to type-B dissections in RAA [9, 32]. In fact, almost all aortic dissection in RAMI cases occurs in the descending aorta [9]. Moreover, AD can increase complications in adults with RAMI because AD in the proximal descending aorta may be directly subject to high abnormal blood flow and cause further abnormal turbulent flow. As a result, RAMI with AD may lead to a higher risk of aneurysm and dissection. Kim *et al.* [33] endorsed proactive surgical resection of AD even in the absence of symptoms, considering the risk of aortic rupture and dissection. On the other hand, RAMI cases with midline descending aorta were accompanied by mild aortic bump in the proximal descending aorta but no AD formation (Fig. 4). The bump might have

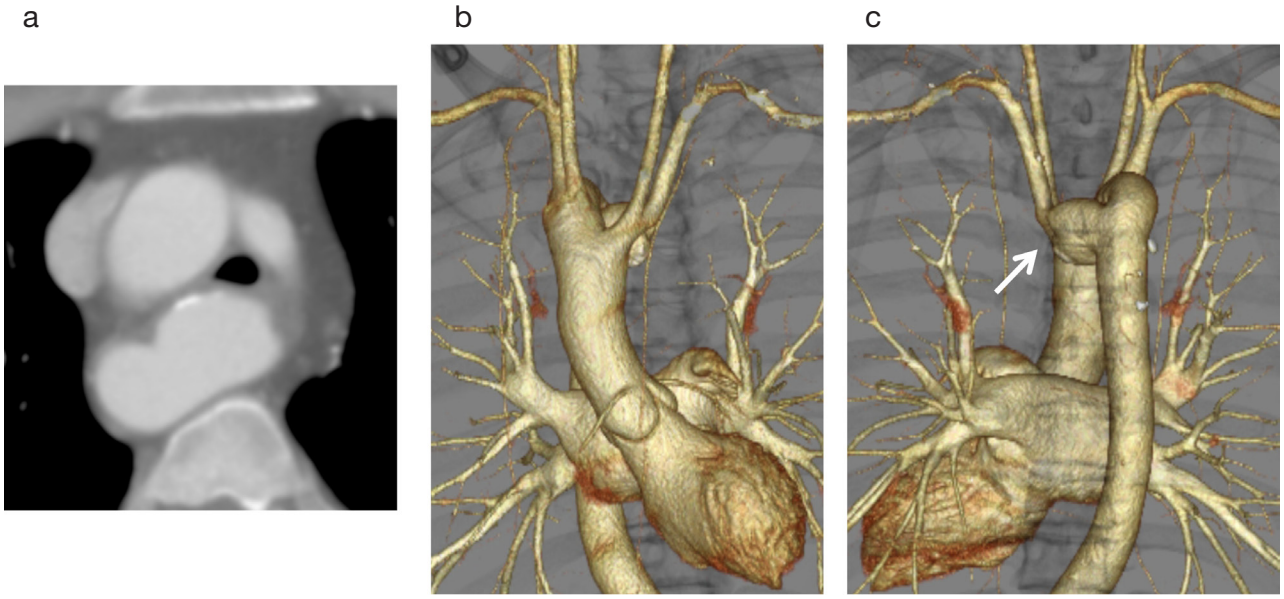

Fig. 3 CT images of an aneurysm involving aortic diverticulum in a 44-year-old male (no. 17 in Table 2).
(a) Axial images of the arterial phase show a snowman-like aneurysm with wall calcification. (b) Anterior view of a 3D image shows RAMI. (c) Posterior view of the 3D image shows an aneurysm involving diverticulum in the proximal descending aorta (arrow).

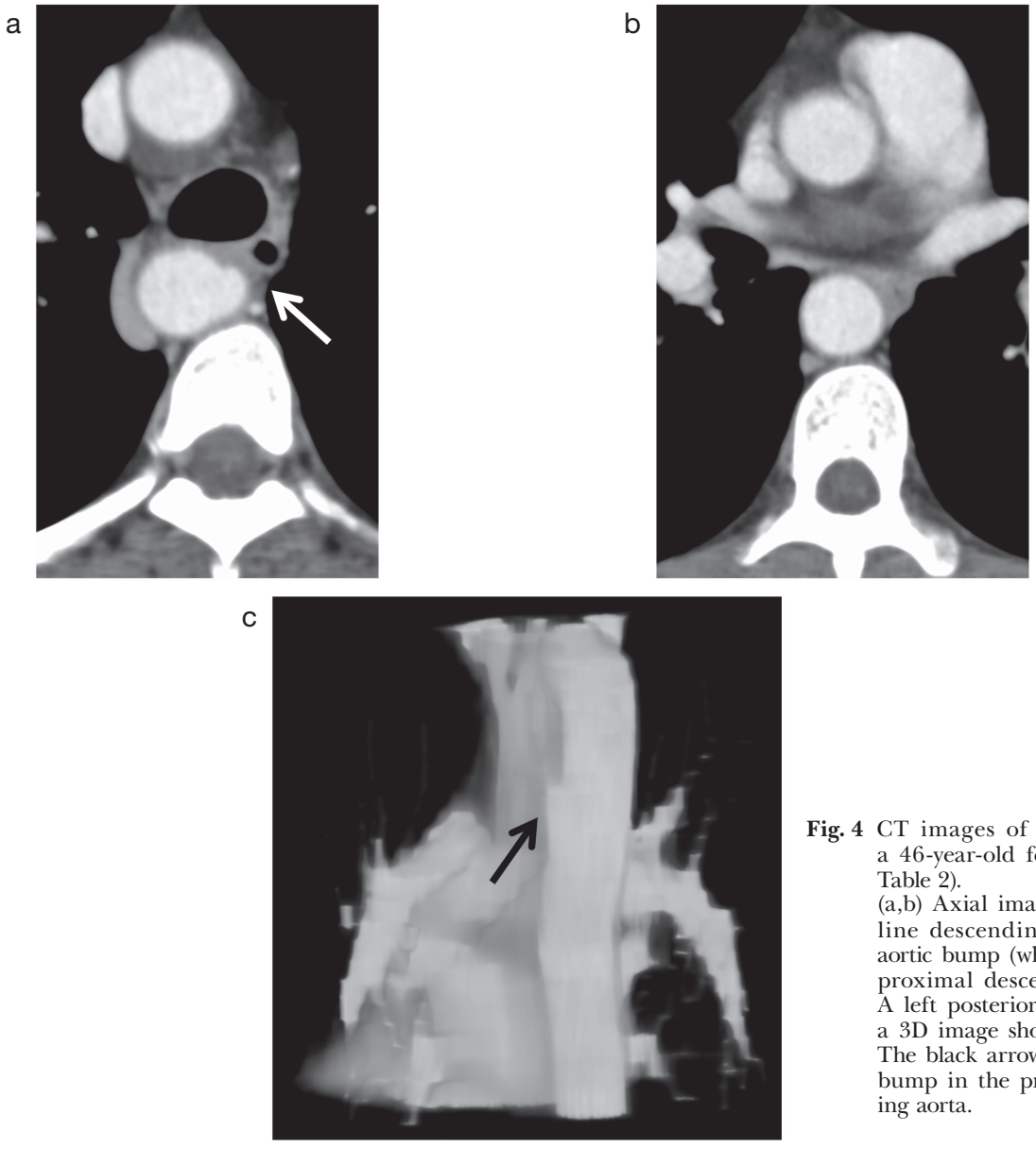

Fig. 4 CT images of aortic bump in a 46-year-old female (no. 18 in Table 2).
(a,b) Axial image showing midline descending aorta and an aortic bump (white arrow) in the proximal descending aorta. (c) A left posterior oblique view of a 3D image showing the RAMI. The black arrow shows an aortic bump in the proximal descending aorta.

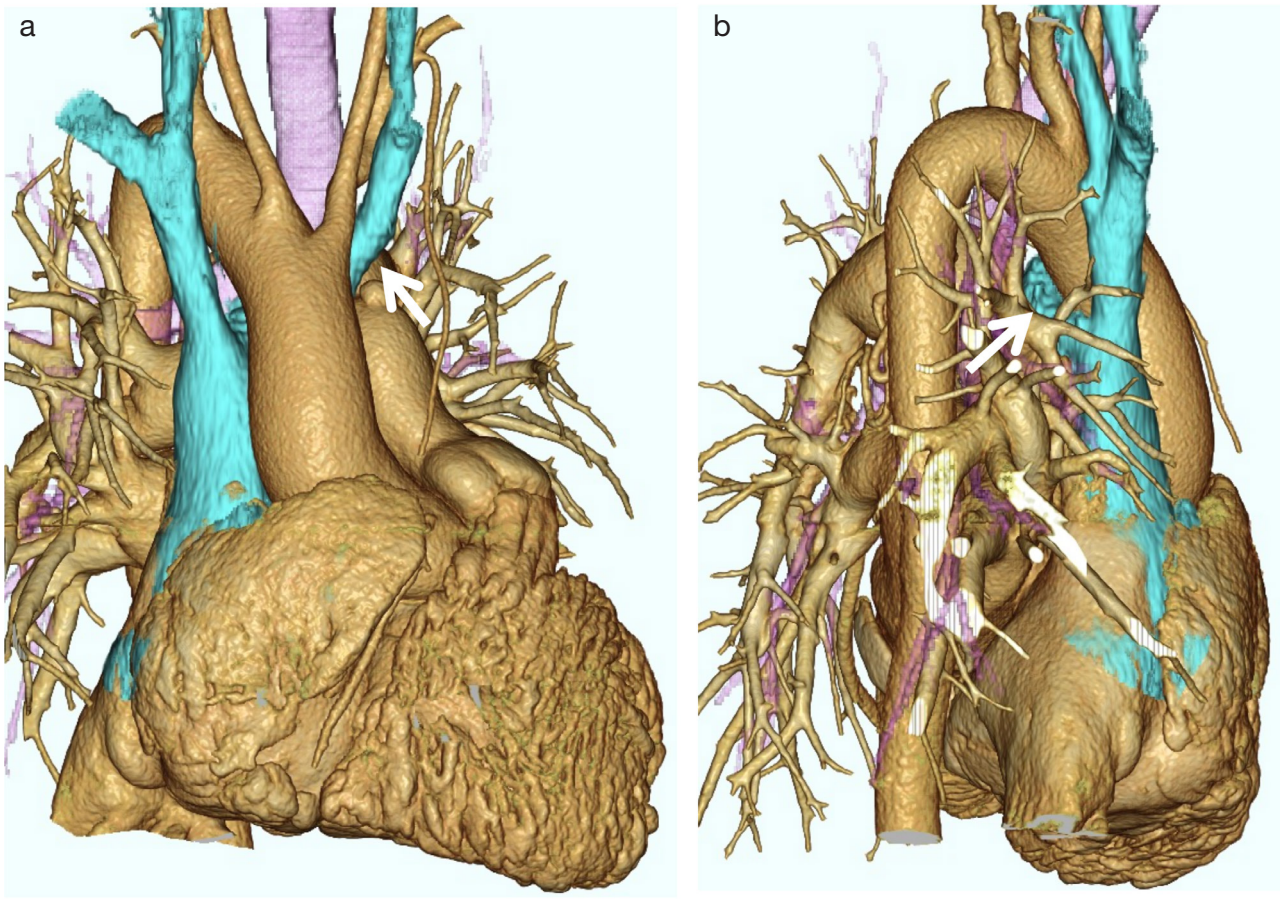

Fig. 5 A case of post-operative tetralogy of Fallot status in a 58-year-old male (no. 15 in Table 2).
(a) Anterior view and (b) right lateral view of 3D-CT images showing RAMI without aortic diverticulum and aberrant left brachiocephalic vein (arrows). The blue line shows the vein. The purple line shows trachea and bronchus.

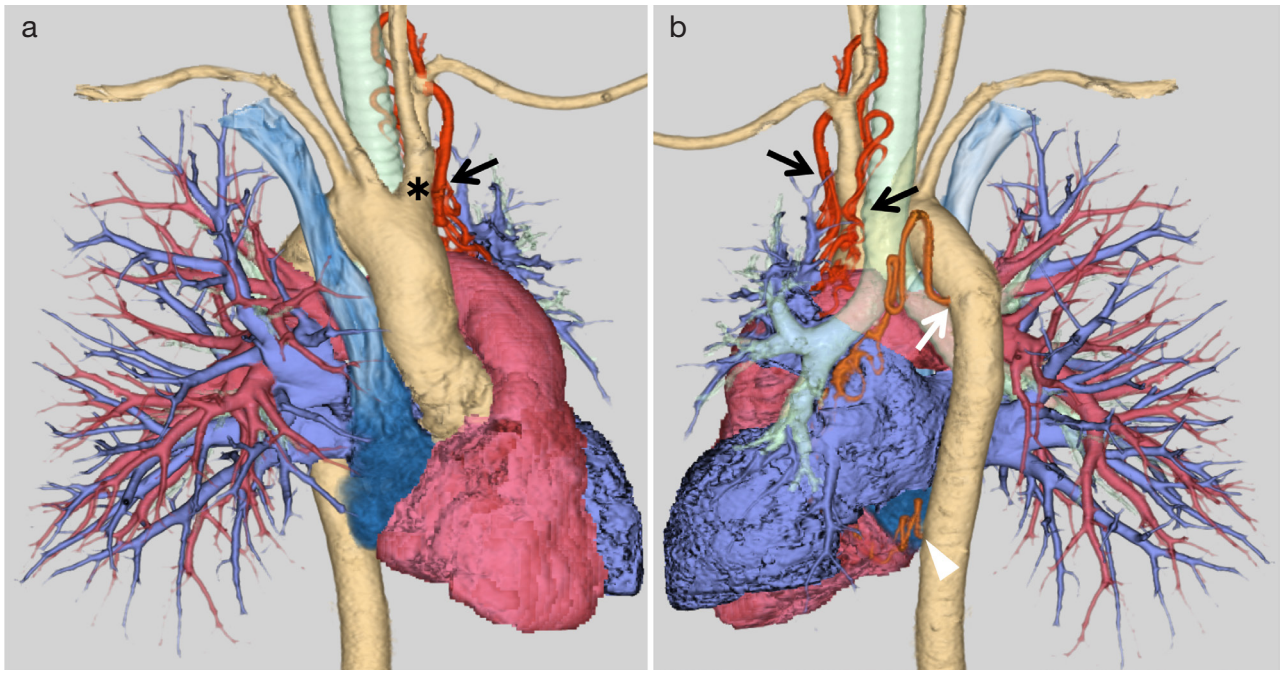

Fig. 6 A case of RAMI associated with an absent left pulmonary artery in a 40-year-old female (no. 23 in Table 2).
3D images (a: right anterior oblique view; b: posterior view) showing RAMI without aortic diverticulum and absent left pulmonary artery. Blue vessels represent the pulmonary veins. The Pink vessels represent the pulmonary arteries. Collateral vessels of the bronchial artery (white arrow) and the anomalous artery (white arrowhead) arising from the descending aorta are seen. Red vessels (black arrows) represent dilated collateral vessels between the pulmonary artery and the left brachiocephalic artery, which are seen in the RAMI. Asterisk: left brachiocephalic artery.

Table 2 Computed tomography findings and clinical data of patients with RAMI

No.	Sex	Age	Level of aortic arch	Shape of proximal DA	Position of DA	Associated congenital CVD	Associated acquired CVD
1	M	84	N	AB	Middle		
2	F	77	H	N	Right		Arteriosclerosis
3	F	71	N	N	Right		
4	M	66	N	N	Right		
5	M	67	N	AD	Right		
6	M	76	H	N	Right		
7	F	56	N	AD	Right		
8	M	43	H	N	Right	TOF, ALBCV	
9	M	26	H	N	Right	TOF	
10	F	53	N	N	Right		
11	M	76	H	AD	Right		Dissecting aneurysm
12	M	35	N	N	Middle		
13	M	65	N	N	Right		
14	F	32	N	N	Right		Stenosis of the LSA
15	M	58	H	N	Right	TOF, ALBCV	
16	M	68	N	AB	Middle	ALBCV	
17	M	44	H	AD	Right		Aortic aneurysm, Arteriosclerosis
18	F	46	N	AB	Middle		
19	F	96	N	N	Right		
20	F	61	N	N	Right		
21	M	90	H	N	Right		
22	M	40	N	N	Right		
23	F	40	N	N	Right	Absence of the PA	
24	F	40	N	N	Right		
25	F	56	N	N	Right		
26	F	77	N	N	Right		
27	F	62	N	N	Right		

RAMI right aortic arch with mirror-image branching, *H* high, *N* normal, *M* male, *F* female, *CVD* cardiovascular disease, *DA* descending aorta, *AB* aortic bump, *AD* aortic diverticulum, *ALBCV* aberrant left brachiocephalic vein, *LSA* left subclavian artery, *TOF* tetralogy of Fallot, *PA* pulmonary artery

been caused due to abnormally high blood pressure from the distal arch to the proximal descending aorta and may have resulted in increased risk of aneurysm and dissection as well as that of AD.

Adult RAMI cases is rarely associated with a vascular ring because the ligamentum arteriosum or the ductus arteriosus is often anteriorly attached to the left brachiocephalic artery [6, 8, 16, 19, 26]. In a few cases, a vascular ring is formed when the ligamentum arteriosum or the ductus arteriosus is attached to the posterior part of the AD and to the pulmonary artery at its anterior end [6, 8, 16, 19, 26]. In our study, among four RAMI cases with AD, two cases showed a symptomatic vascular ring due to complicated AD, and the other two cases with AD and right-sided descending aorta did not show symptomatic vascular ring formation probably because of large separation between the AD and the left brachiocephalic artery.

IDA is a subtype of a double aortic arch and the double aortic arch with atresia of the distal left arch segment. One of the characteristics of this anomaly is AD in the descending aorta [2, 26]. IDA is an anomaly basically different from RAMI in that the left sided aortic arch has continuity to the right sided aortic arch with a fibrous cord. Nevertheless, it is difficult to differentiate between IDA and RAMI, because the fibrous cord is very small and configurations of IDA and RAMI with AD are very similar. There are several clues indicating IDA rather than RAMI (Table 1). IDA cases have symmetric subclavian and common carotid arteries originating from the aortic arch. In contrast, RAMI is indicated by a more anterior position of the left subclavian artery [26]. Schlesinger *et al.* have identified a long tubular diverticulum in IDA cases [26]. In our study, we found no tubular diverticula.

Previous studies have reported that RAMI is rare and is the second most common anomaly in RAA. However, the exact incidence of RAMI in the general population is unclear [15, 18]. To the best of our knowledge, our study was the first to address incidence of RAMI, and we found that RAMI cases detected in CT examinations represented less than 2 out of 10,000 adults. The 27 RAMI cases we studied included post-operative CHD cases and RAMI cases with or without congenital vascular disease found incidentally on CT. There have been some case reports of complicated and/or operative AD in adults [7, 12, 23, 24]. In our study, the patient with the largest dissecting-AD aneurysm was followed-up because of a lack of change in aneurysm size and mild symptoms (Fig. 2). Another case with an AD aneurysm was operated on due to a symptomatic vascular ring (Fig. 3). In addition, a case of absent left pulmonary artery was found incidentally (Fig. 6). McElbinney *et al.* [6] reported that in RAMI without CHD, associated absent left pulmonary artery and vascular ring were not very rare.

Our study had several limitations. First, the sample size of RAMI cases detected in CT was rather small.

There was no case with left-sided descending aorta (retroesophageal descending aorta) in our study. A large study involving surgical cases or autopsy series is needed to determine the true incidence of RAMI and evaluate clinical significance in adulthood. Second, some cases of RAMI might not have been detected because we used a keyword-based search of CT reports to identify cases. Third, we did not evaluate the effect of blood flow on the aortic wall using CFD in RAMI cases. Finally, CHD was investigated using only medical records, and an echocardiographic exam or angiography is needed to determine and verify its existence.

Surgery of anomalous aortic arch involving RAA is very complex [3, 9, 12, 23, 27]. In most previous studies, open aortic surgery was often chosen due to RAMI. In a recent study, endovascular aortic repair was performed due to its less invasive nature and fewer complications; a hybrid aortic repair of an aortic aneurysm with RAMI including AD has been also reported [23]. Emergency surgery due to aortic dissection or rupture in RAA appears to be a higher risk than that in LAA. Thus, it may be necessary to consider an earlier stage for treatment of RAMI with AD or aneurysms, even though asymptomatic.

In conclusion, adults with RAMI identified in CT examinations were extremely rare. Among 27 adults with RAMI, three patients were associated with TOF. Almost all RAMI cases were asymptomatic except two cases showing vascular ring formation due to AD. RAMI without CHD is considered a benign condition by most radiologists. However, adults with RAMI may have increased risk of acquired aortic disease and should be monitored carefully and if necessary, proactive treatment should be considered.

REFERENCES

1) Holland P, Fitzpatrick JD. Case report: magnetic resonance imaging of a right-sided cervical aortic arch with a congenital aneurysm. Clin Radiol. 1991; 43: 352–5.
2) Kanne JP, Godwin JD. Right aortic arch and its variants. J Cardiovasc Comput Tomogr. 2010; 4: 293–300.
3) Ichikawa T, Koizumi J, Tanno K, Okochi T, Nomura T, Shimura S, *et al*. Kommerell Diverticulum in Adults: Evaluation of Routine CT Examinations. Tokai J Exp Clin Med. 2016; 41: 65–9.
4) Hastreiter AR, D'Cruz IA, Cantez T. Right-sided aorta. Part I. Occurrence of right aortic arch in various types of congenital heart disease. Br Heart J. 1966; 28: 722–5, 737–9.
5) Knight L, Edwards JE. Right aortic arch. Types and associated cardiac anomalies. Circulation. 1974; 50: 1047–51.
6) McElhinney DB, Hoydu AK, Gaynor JW, Spray TL, Goldmuntz E, Weinberg PM. Patterns of right aortic arch and mirror-image branching of the brachiochephalic vessels without associated anomalies. Pediatr Cardiol. 2001; 22: 285–91.
7) Shingu Y, Shiiya N, Matsuzaki K, Kunihara T, Matsui Y. Dysphagia due to aortic diverticulum: an adult surgical case. Ann Thorac Cardiovasc Surg. 2007; 13: 132–4.
8) Higashikuni Y, Nagashima T, Isizaka N, Kinugawa K, Hirata Y, Nagai R. Right aortic arch with mirror image branching and vascular ring. Int J Cardiol. 2008; 130: e53–5.
9) Kaneda T, Lemura J, Zhang Z, Inoue T, Onoe M, Kitayama H, *et al*. A case of Stanford type B aortic dissection involving a right-sided aortic arch with mirror-image branching and right-sided descending aorta. Thorac Cardiovasc Surg. 2001; 49: 51–3.
10) Khitin L, Kim K, Phillips KD, Ikonomidis JS. An aneurysm of right-sided aortic arch with mirror-image brachiocephalic branching. J Thorac Imaging. 2005; 20: 307–9.
11) Grathwohl KW, Afifi AY, Dillard TA, Olson JP, Heric BR. Vascular rings of the thoracic aorta in adults. Am Surg. 1999; 65: 1077–83.
12) Harada S, Nakamura Y, Marumoto A, Saiki M, Ishiguro S, Nishimura M. A surgical case of Kommerell's diverticulum with a right-sided aortic arch. Jpn J Cardiovasc Surg. 2009; 38: 368–71 **(in Japanese)**.
13) Garti IJ, Aygen MM, Vidine B, Levy MJ. Right aortic arch with mirror-image branching causing vascular ring. A new classification of the right aortic arch patterns. Br J Radiol. 1973; 46: 115–9.
14) Edwards JE. Anomalies of derivatives of the aortic arch system. Med Clin North Am. 1948; 32: 925–49.
15) Stewart JR, Owings W, Kincaid OW, Edwards JE. An Atlas of Vascular Rings and Related Malformation of the Aortic Arch System. Charles C Thomas, Springfield, Illinois, 1964.
16) Hanneman K, Newman B, Chan F. Congenital Variants and Anomalies of the Aortic Arch. Radiographics. 2017; 37: 32–51.
17) Oddone M, Granata C, Vercellino N, Bava E, Tomà P. Multimodality evaluation of the abnormalities of the aortic arches in children: techniques and imaging spectrum with emphasis on MRI. Pediatr Radiol. 2005; 35s: 947–60.
18) Ramos-Duran L, Nance JW Jr, Schoepf UJ, Henzler T, Apfaltrer P, Hlavacek AM. Developmental aortic arch anomalies in infants and children assessed with CT angiography. AJR Am J Roentgenol. 2012; 198: W466–74.
19) D'Souza VJ, Velasquez G, Galss TA, Formanek AG. Mirror-Image right aortic arch: a proposed mechanism in symptomatic vascular ring. Cardiovasc Intervent Radiol. 1985; 8: 134–6.
20) Subramaniam KG, Grant PW. Vascular ring: right aortic arch, mirror image branching with Kommerell's diverticulum. Heart Lung Circ. 2010; 19: 56–7.
21) Zachary CH, Myers JL, Eggli KD. Vascular ring due to right aortic arch with mirror-image branching and left ligamentum arteriosus: complete preoperative diagnosis by magnetic resonance imaging. Pediatr Cardiol. 2001; 22: 71–3.
22) Ryu JW. Complete vascular ring caused by Kommerell's diverticulum and right aortic arch with mirror image branching. Korean J Thorac Cardiovasc Surg. 2012; 45: 338–41.
23) Sato S, Matsuda H, Fukuda T, Domae K, Iba Y, Tanaka H, *et al*. Hybrid repair combined with open surgery and endografting for lesions in right aortic arch:report of three cases. Ann Vasc Dis. 2012; 5: 61–4.
24) Fadel E, Chapelier AR, Cerrina J, Macchiarini P, Dartevelle PG. Vascular ring causing symptomatic tracheal compression in adulthood. Ann Thorac Surg. 1995; 60: 1411–3.
25) Greiner A, Perkmann R, Reiger M, Neuhauser B, Fraedrich G. Vascular ring causing tracheal compression in an adult patient. Ann Thorac Surg. 2003; 75: 1959–60.
26) Schlesinger AE, Krishnamurthy R, Sena ML, Guillerman RP, Chung T, DiBardino DJ, *et al*. Incomplete double aortic arch with atresia of the distal left arch: distinctive imaging appearance. AJR Am J Roentgenol. 2005; 184: 1634–9.
27) Kim SH, Chung JW, Im JG, Choi YW, Choe YH, Han MC. Subaortic left innominate vein: radiologic findings and consideration of embryogenesis. J Thorac Imaging. 1999; 14: 142–6.
28) Isselbacher EM. Thoracic and abdominal aortic aneurysms. Circulation. 2005; 111: 816–28.
29) McMahon MA, Squirrell CA. Multidetector CT of Aortic Dissection: A Pictorial Review. Radiographics. 2010; 30: 445–60.
30) Ahmad F, Cheshire N, Hamady M. Acute aortic syndrome: pathology and therapeutic strategies. Postgrad Med J. 2006; 82: 305–12.
31) Numata S, Itatani K, Kanda K, Doi K, Yamazaki S, Moritomo K, *et al*. Blood flow analysis of the aortic arch using computational fluid dynamics. Eur J Cardiothorac Surg. 2016; 49: 1578–85.
32) Bodine JA, D'Souza VJ, Formanek AG. An unusual type of dissecting thoracic aneurysm in association with right aortic arch. VASA J Vasc Dis. 1982; 11: 223–8.
33) Kim KM, Cambria RP, Isselbacher EM, Baker JN, LaMuraglia GM, Stone JR, at al. Contemporary surgical approaches and outcomes in adults with Kommerell diverticulum. Ann Thorac Surg. 2014; 98: 1347–54.